

Numerical simulation study on response characteristics of the different geological models of mine full-space transit electromagnetism

In this paper, it builds the geological simulations models for low resistance abnormality, high resistance abnormality, water flowing fault, water flowing subsided column, water accumulating gob and non-water accumulating gob according to the mine full-space transmit electromagnetic detection theory and by aiming at the several main water inrush structures of mine. Moreover, it gives numerical simulation to full-space transit electromagnetic responses of the several models above by utilizing MATLAB software, and the analytical research results indicate that the mine transit electromagnetism can distinguish the low resistance abnormality more obvious and the high resistance abnormality slightly inferior, especially that simulation detection curve of the water accumulating gob is more obvious. Simultaneously, the induced voltage corresponding to the low-resistance reaction is represented as high potential, and that corresponding to the high-resistance reaction is represented as low potential, and this trend is basically same as that of the half space.

Keywords: Mine full-space transmit electromagnetism, response characteristics, geological model, numerical simulation.

1. Introduction

Along with increment and expansion of the coal mining depth, strength, speed and scale, coal mine shows water inrush accidents frequently affects seriously and restricts safety in production of the coal mine. How to control damage of water inrush becomes the primary consideration for safety in production of coal mine, and mine transmit electromagnetic method can solve the water damage detection problem effectively. However, there are few relevant research achievements as to the response characteristics of the different geological models of underground full-space

small coils. This paper shall give numerical simulation study on the full-space response characteristics by utilizing the geological model for water inrush structure already built and by aiming at main structures of mine water inrush, e.g. water flowing fault, water-bearing karst, water-enriched subsided column and abandoned mine water[1].

2. Mine full-space transient electromagnetic detection principle

When conducting transient electromagnetic detection in mine tunnel, the full-space electromagnetic response shall be obtained, while it is not applicable to the half-space theory on ground, and the detection principle is as shown in Fig.1. Before the current is switched off (when $t < 0$), the emission current shall build a stable magnetic field surrounding the loop and in the tunnel, as shown in formula (1):

$$I(t) = \begin{cases} I & t < 0 \\ 0 & t \geq 0 \end{cases} \quad \dots 1$$

When switching off the emission current at the moment $t = 0$, the primary magnetic field generated by emission current shall disappear immediately, and the acute change of the primary magnetic field shall motivate induced current in the surrounding rock of tunnel to maintain the magnetic field existed before, thus the induced magnetic field as shown in Fig.2 shall be generated. For ohmic loss of the surrounding rock of the mine tunnel, the magnetic field generated by induced current shall show rapid damping, and the magnetic field damped rapidly shall again induce new eddy current (secondary magnetic field) with weaker strength in the surrounding underground medium. Thus, we can give detection and explanation to the front rock stratum in tunnel by utilizing this characteristic of the secondary magnetic field and measuring change of the induced voltage [1-2].

As that widely used in the mine currently is magnetic coupling-source transient electromagnetic method, the induced voltage of the secondary magnetic field received by adopting full-space transient electromagnetic method is as shown in the formula (2) [4-7]:

$$V_z(t) = -q \frac{\partial B_z(t)}{\partial t} = \frac{Mq\mu^{5/2}\sigma^{3/2}}{8\pi^{3/2}t^{5/2}} \quad \dots 2$$

Messrs. Jun Zhang, Key Laboratory of Metallogenic Prediction of Nonferrous Metals and Geological Environment Monitoring (Central South University), Ministry of Education, Changsha 410083, China, Yunbo Li, School of Geosciences and Info-Physics, Central South University, Changsha 410083, China and Xifang Tian Chongqing Research Institute of China Coal Technology & Engineering Group Corp, Chongqing 400039, China. Email: lyb0112@163.com

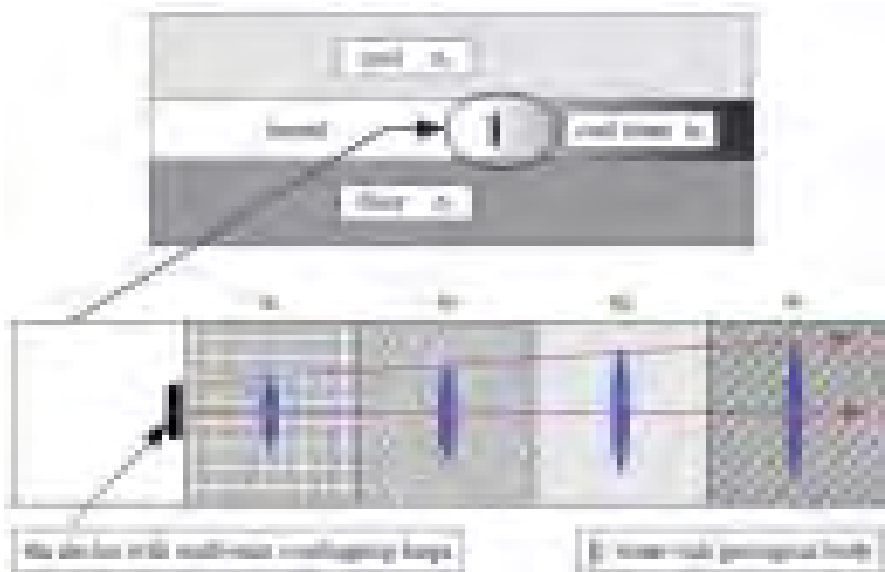


Fig.1 Mine transient electromagnetic detection principle

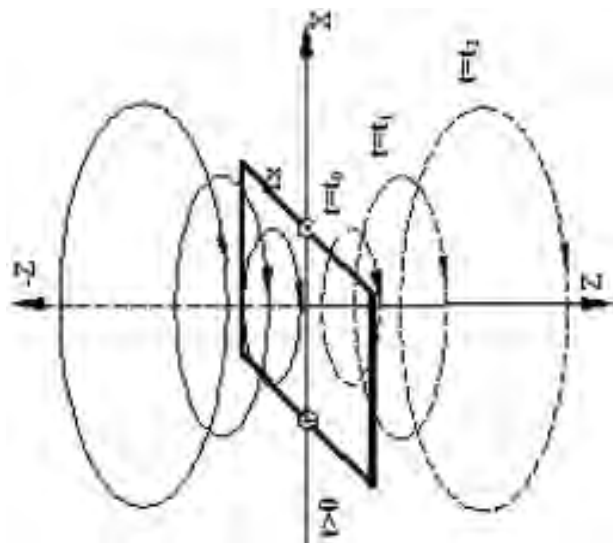


Fig.2 Underground magnetic field distribution of the transient electromagnetic method

In the formula, when emission loop area is S , number of turns is N , and supply current intensity is I , magnetic coupling distance of emission loop shall be $M = S \times N \times I$; when reception loop area is s , and number of turns is n , effective area of the reception loop shall be $q = s \times n$. $\mu = \mu_0 = 4\pi \times 10^{-7} \text{h/m}$ refers to magnetic conductivity of air, and σ refers to electric conductivity.

3. Simulation on response characteristics of the different geological models of full-space small coils

Mine water inrush structures mainly include water flowing fault, water-bearing karst, water-enriched subsided column and abandoned mine water, etc. which can be simulated by such low resistance

models as nearly erect thin pulse, cylinder and sphere respectively. In this paper, it uses the several geological models as shown in Table 1 in researching transient electromagnetic response characteristics of the full-space small coils.

Model 1 is low resistance abnormality model. It adopts full-space model and uses Matlab simulation according to the full-space transient electromagnetic theory, emission current $I=2\text{A}$ of the overlapping loop is used in the calculation, number of turns of the emission coil is ten, and that of the reception coil is twenty, size of the coil is 1.5m, and model parameters are as shown in Fig.3.

The simulated calculation results are as shown in Fig.4, and it can be seen from the results that induced voltage shall increase, resolution capacity shall be stronger and detection effect shall be more obvious when detecting from high resistance abnormality to low resistance abnormality.

TABLE 1. MAIN PARAMETERS OF THE GEOLOGICAL MODELS

Model	Parameters
Model 1: Low resistance abnormality model	Half space of the left half part $\rho=100\Omega \cdot \text{m}$, the first layer of the right half part $\rho=100\Omega \cdot \text{m}$, $h=30\text{m}$, the second layer $\rho=10\Omega \cdot \text{m}$, $h=30\text{m}$, the third layer $\rho=100\Omega \cdot \text{m}$
Model 2: High resistance abnormality model	Half space of the left half part $\rho=10\Omega \cdot \text{m}$, the first layer of the right half part $\rho=10\Omega \cdot \text{m}$, $h=30\text{m}$, the second layer $\rho=100\Omega \cdot \text{m}$, $h=30\text{m}$, the third layer $\rho=10\Omega \cdot \text{m}$
Model 3: Water flowing fault	Half space of the left half part $\rho=100\Omega \cdot \text{m}$, the first layer of the right half part $\rho=100\Omega \cdot \text{m}$, $h=30\text{m}$, the second layer $\rho=10\Omega \cdot \text{m}$, width of the fault fracture zone $h=3\text{m}$, the third layer $\rho=100\Omega \cdot \text{m}$
Model 4: Water flowing subsided column	Half space of the left half part $\rho=100\Omega \cdot \text{m}$, the first layer of the right half part $\rho=100\Omega \cdot \text{m}$, $h=30\text{m}$, the second layer $\rho=10\Omega \cdot \text{m}$, diameter of the subsided column 10m, the third layer $\rho=100\Omega \cdot \text{m}$
Model 5: Water accumulating gob	Half space of the left half part $\rho=100\Omega \cdot \text{m}$, the first layer of the right half part $\rho=100\Omega \cdot \text{m}$, $h=30\text{m}$, water accumulation in gob of the second layer $\rho=10\Omega \cdot \text{m}$
Model 6: Non-water accumulating gob	Half space of the left half part $\rho=100\Omega \cdot \text{m}$, the first layer of the right half part $\rho=100\Omega \cdot \text{m}$, $h=30\text{m}$, non-water accumulating gob of the second layer $\rho=10^6\Omega \cdot \text{m}$



Fig.3 Simulated calculation model of low resistance abnormality

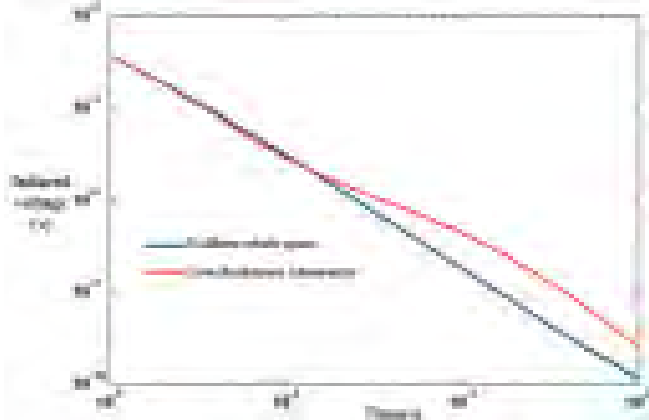


Fig.4 Simulated calculation results of low resistance abnormality

Model 2 is high resistance abnormality model. It adopts full-space model and uses Matlab simulation according to the full-space transient electromagnetic theory, emission current $I=2A$ of the overlapping loop is used in the calculation, number of turns of the emission coil is ten, and that of the reception coil is twenty, size of the coil is 1.5m, and model parameters are as shown in the Fig.5.

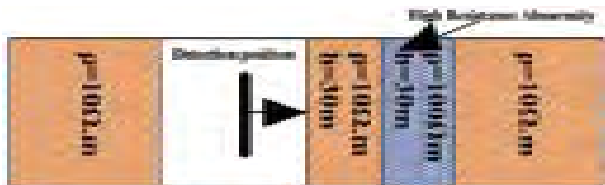


Fig.5 Simulated calculation model of high resistance abnormality

The simulated calculation results are as shown in Fig.6, and it can be seen from the results that induced voltage shall decrease, relative resolution capacity shall be weak and detection effect shall be not too obvious when detecting from low resistance abnormality to high resistance abnormality.

Model 3 is water flowing fault model, and it is used in simulating the full-space transient electromagnetic reaction in the condition that width of the fault fracture zone is 3m. It adopts full-space model and uses Matlab simulation according to the full-space transient electromagnetic theory, emission current $I=2A$ of the overlapping loop is used in the calculation, number of turns of the emission coil is ten, and that of the reception coil is twenty, size of the coil is 1.5m, and model parameters are as shown in the Fig.7.

The simulated calculation results are as shown in Fig.8,

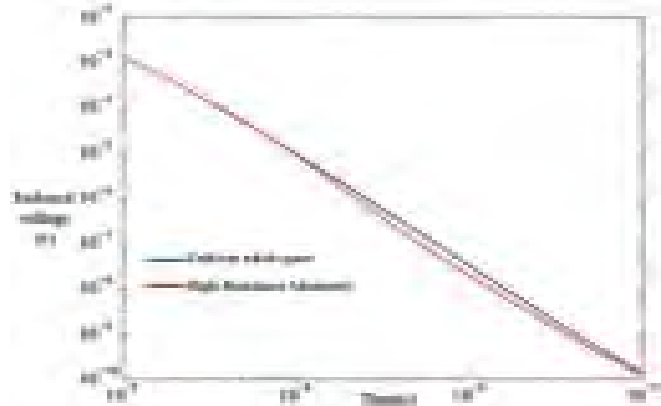


Fig.6 Simulated calculation results of high resistance abnormality

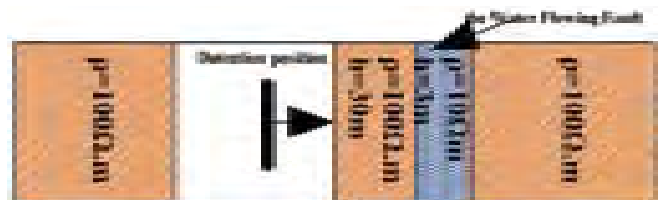


Fig.7 Simulated calculation model of the water flowing fault

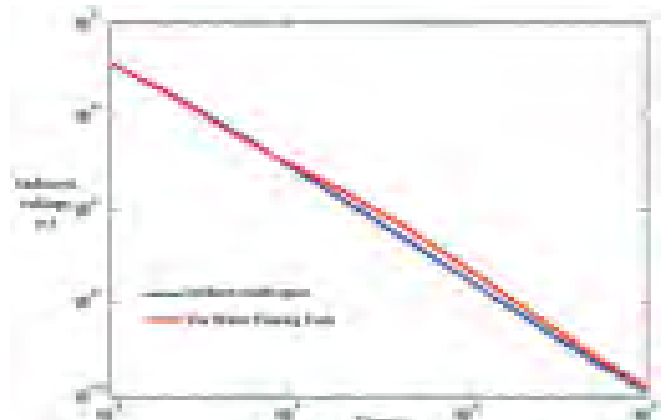


Fig.8 Simulated calculation results of the water flowing fault

and it can be seen from the results that induced voltage reaction of the water flowing fault shows high potential and the potential tends to normal potential gradually after passing the fault, which reflects the feasibility of detecting water flowing of fault with full-space transient electromagnetic method.

Model 4 is water flowing subsided column model, and diameter of the water flowing subsided column is 10m. It adopts full-space model and uses Matlab simulation according to the full-space transient electromagnetic theory, emission current $I=2A$ of the overlapping loop is used in the calculation, number of turns of the emission coil is ten, and that of the reception coil is twenty, size of the coil is 1.5m, and model parameters are as shown in Fig.9.

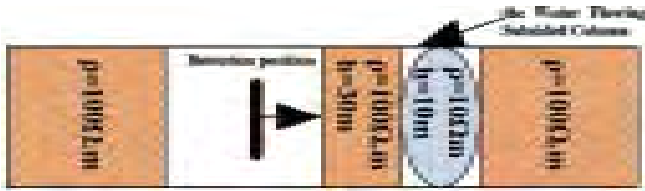


Fig.9 Simulated calculation model of the water flowing subsided column

The simulated calculation results are as shown in Fig.10, and it can be seen from the results that induced voltage reaction of the water flowing subsided column shows high potential, which is more obvious than the water flowing fault reaction, has relation with the diameter of subsided column and reflects the feasibility of detecting water flowing of subsided column with full-space transient electromagnetic method.

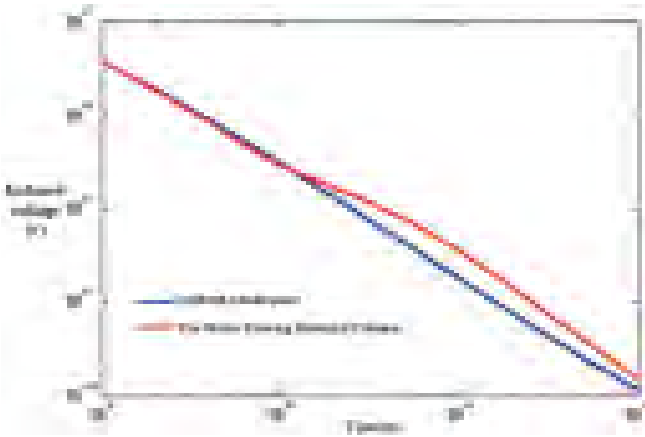


Fig.10 Simulated calculation results of the water flowing subsided column

Model 5 is water accumulating model for gob, and it is used in simulated detection of the water accumulation in the gob after 30m forward the coal layer. It adopts full-space model and uses Matlab simulation according to the full-space transient electromagnetic theory, emission current $I = 2A$ of the overlapping loop is used in the calculation, number of turns of the emission coil is ten, and that of the reception coil is twenty, size of the coil is 1.5m, and model parameters are as shown in Fig.11.

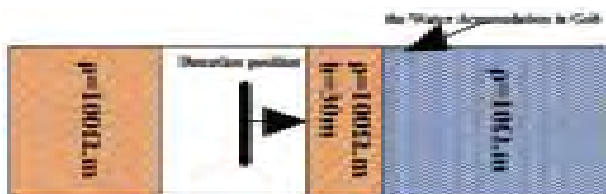


Fig.11 Simulated calculation model of the water accumulation in gob

The simulated calculation results are as shown in Fig.12, and it can be seen from the results that induced voltage reaction of the water accumulation in gob shows high potential and water accumulating reaction of gob is more

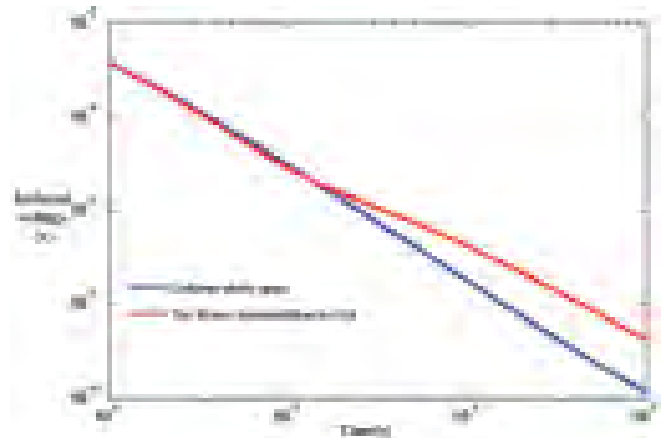


Fig.12 Simulated calculation results of the water accumulation in gob obvious by relatively speaking, which has relation with the large-area water accumulation in gob and reflects the feasibility of detecting water accumulation in gob with full-space transient electromagnetic method.

Model 6 is non-water accumulating model for gob, and it is used in simulated detection of the non-water accumulation in the gob after 30m forward the coal layer. It adopts full-space model and uses Matlab simulation according to the full-space transient electromagnetic theory, emission current $I=2A$ of the overlapping loop is used in the calculation, number of turns of the emission coil is ten, and that of the reception coil is twenty, size of the coil is 1.5m, and model calculation parameters are as shown in Fig.13.



Fig.13 Simulated calculation model of the non-water accumulation in gob

The simulated calculation results are as shown in Fig.14, and it can be seen from the results that induced voltage reaction of the non-water accumulation in gob shows low

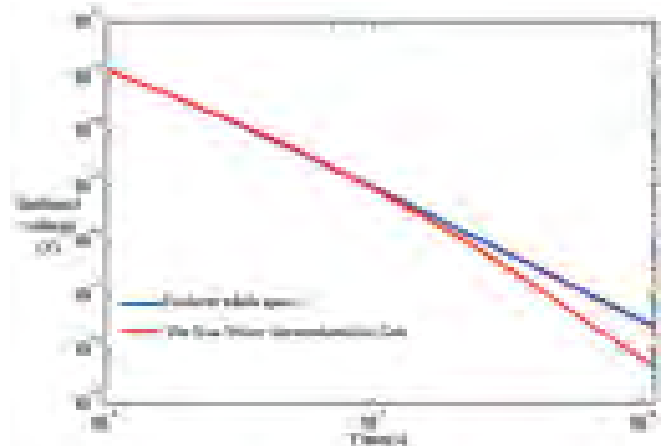


Fig.14 Simulated calculation results of the non-water accumulation in gob

potential and non-water accumulating reaction of gob is more obvious by relatively speaking, which reflects the feasibility of detecting non-water accumulation in gob with full-space transient electromagnetic method.

3. Conclusions

It is known from the numerical simulation analysis on the different geological models of the mine full-space small coil transient electromagnetism that:

1. The mine transit electromagnetism can distinguish the low resistance abnormality more obvious and the high resistance abnormality slightly inferior, so mine transit electromagnetism is generally used in detecting the underground low resistance abnormality, and it gives detection by mainly aiming at water-bearing body of the mine, including water flowing fault, water flowing subsided column and water accumulating gob, etc. The simulated detection curve of water accumulating gob is more obvious, which provides the technical means for solving the water accumulation in abandoned mine and gob.
2. Simultaneously, it can be seen that the induced voltage corresponding to the low-resistance reaction is represented as high potential, and that corresponding to the high-resistance reaction is represented as low potential, and this law is same as that of the ground half space.

acknowledgment

The project is supported by National Science and Technology Major Project of the Ministry of Science and Technology of China (Grant No. 2016ZX05045-002-0003).

References

- [1] Lin, J., Wang, L., Wang, X., Cao, M., Fu, L., Shang X. (2016): "Research and development on the air-core coil sensor for mine transient electromagnetic exploration," *Chinese Journal of Geophysics*, vol.59, no.2, pp.721-730.
- [2] Cheng, J.L., Chen, D., Xue, G.Q., Qiu, H., Zhou, X.T. (2016): "Synthetic aperture imaging in advanced detection of roadway using the mine transient electromagnetic method," *Chinese Journal of Geophysics*, vol.59, no.2, pp.731-738
- [3] Oristaglio, M.L., Hohmann, G.W. (1984): "Diffusion of electromagnetic fields in two-dimensional earthy finite-difference approach," *Geophysics*, no.49, pp.870-894.
- [4] Gerrit, M. (1998): "Total-Field Absorbing Boundary Conditions for the Time-Domain Electromagnetic Field Equations," *IEEE Trans. on Electromagnetic Compatibility*, vol. 40, no.5, pp.100-102.
- [5] Wait, J.R. (1951): "Transient EM propagation in a conducting medium," *Geophysics*, no.16, pp.213-221.
- [6] Nabighian, M.N. (1979): "Quasi-static transient response of a conducting half-space-An approximate representation," *Geophysics*, no. 44, pp. 1700-1705.
- [7] Kuo, J.T., Cho, D.H. (1980): "Transient time-domain electromagnetic," *Geophysics*, no.45, pp. 271-292.
- [8] Yin, C., Smith, R.S., Hodges, G., Annan, P. (2008): "Modeling results of on-and off-time B and dB/dt for time-domain airborne EM system," 70th EAGE Conference and Exhibition, Extended Abstract, H048.
- [9] Xu, Y.C., Wang, Y. et al. (2011): "Development of High Resolution and Low Noise Transient Electromagnetic Receiver," 2011 International Conference on Electric Information and Control Engineering, vol.7, pp.5839-5842.
- [10] Reid, J.E., Macnaez, J.C. (2002): "Resistive limit modeling of air-borne electromagnetic data," *Geophysics*, vol. 67, no. 2, pp. 492-500.
- [11] Mith, R.S., Balch, S.J. (2000): "Robust estimation of band limited inductive limit response from impulse-response TEM measurements taken during the transmitter switch-off and the transmitter off-time: theory and an example from Voisey's Bay, Labrador, Canada," *Geophysics*, vol. 65, no. 2, pp. 476-481.
- [12] Svllans, M. (2006): "Quantitative interpretation of responses of Helicopter borne concentric loop EM geophysical survey systems [Bachelor of Science]," Ottawa, Ontario: Carleton University Earth Sciences.
- [13] Baleh, S.J., Boyko, W.P., Paterson, N.R. (2003): "The Aero TE Mairborne electromagnetic system," *The Leading Edge*, vol.22, no.6, pp.562-566.
- [13] Liu X.A., and Jia C.Q. (2004): "Multimedia equivalence model of chemical fate of heavy metal pollution in three-gorges valley," *Computers & Applied Chemistry*, vol.21, no.2, 299-304.
- [14] Wang X.L., Wang M.H., Quan S.X., Yan B., and Xiao X.M. (2016): "Influence of thermal treatment on fixation rate and leaching behavior of heavy metals in soils from a typical e-waste processing site," *Journal of Environmental Chemical Engineering*, vol. 4, no.1, pp.82-88.
- [15] Cannistraro G., Cannistrar M., and Restivo R., "Some observations on the radiative exchanges influence on thermal comfort in rectangular open-space environments," *International Journal of Heat and Technology*, vol.33, no.2, pp.79-84, 2015.
- [16] Gattuso D., Greco A., Marino C., Nucara A., Pietrafesa M., and Scopelliti F. (2016)? "Sustainable mobility: environmental and economic analysis of a cable railway, powered by photovoltaic system," *International Journal of Heat and Technology*, vol.34, no.1, pp.7-14.

RESEARCH ON ENVIRONMENTAL CHEMICAL BEHAVIOUR OF HEAVY METALS IN ATMOSPHERIC DUSTFALL

Continued from page 723